*Kirk-Othmer Encyclopedia of Chemical Technology.*


# FRACTURE MECHANICS

Fracture mechanics is a methodology which characterizes the resistance of a material to crack propagation. Provided specific requirements are met, a material property can be measured which describes the performance of the material when a sharp or natural crack is present. This property is called the plane strain fracture toughness and is independent of the specimen geometry used to make the measurement. The measured fracture toughness can then be used in the design of a component or structure to avoid fracture. The concepts of fracture mechanics for brittle crack growth were originally proposed in 1920 (1–3). However, it was not until World War II that the technology was substantially developed. Crack propagation problems were experienced with the Liberty ships constructed to carry supplies across the Atlantic ocean. Over a hundred ships fractured in half and many others had serious cracks, leading to extensive research into brittle fracture in metals. Later, the development of nuclear power plants and other critical structures made accurate predictions of the fracture behavior of thick-walled metal parts essential.

Fracture mechanics is now quite well established for metals, and a number of ASTM standards have been defined (4–6). For other materials, standardization efforts are underway (7, 8). The techniques and procedures are being adapted from the metals literature. The concepts are applicable to any material, provided the structure of the material can be treated as a continuum relative to the size-scale of the primary crack. There are many textbooks on the subject covering the application of fracture mechanics to metals, polymers, and composites (9–15) (see Composite materials).

## 1. Inherent Flaws

Perhaps the single most important concept in fracture mechanics is the existence of inherent flaws. Any material contains imperfections or defects. Examples are voids at grain boundaries in metals or a dirt particle in a polymer. It is from these defects that cracks eventually begin to grow, because defects cause local stress concentrations. A structure having no defects would not fracture. A structure having a large defect fractures at a lower load than an otherwise identical structure containing a smaller defect. Therefore, fracture is controlled by both the defect size, effectively the length of the crack already present, and the magnitude of the load which can be applied before failure occurs. The most severe defect is a sharp crack because this causes the most severe stress concentration. Fracture mechanics describes the different combinations of applied load and defect size which can lead to failure in a body containing a sharp crack.

## 2. Linear Elastic Fracture Mechanics

A crack in a body may grow as a result of loads applied in any of the three coordinate directions, leading to different possible modes of failure. The most common is an in-plane opening mode (Mode I). The other two are

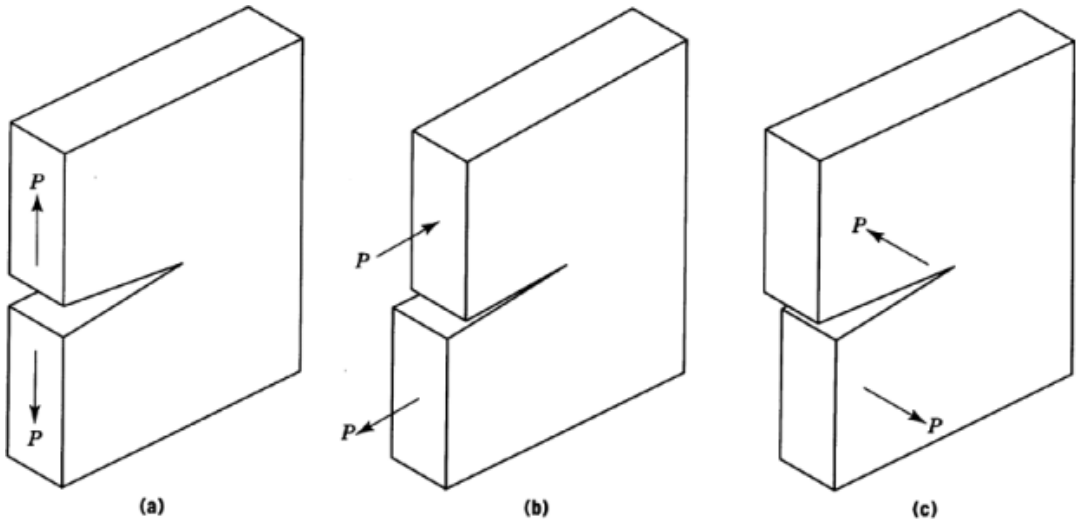


**Fig. 1.** Three modes of fracture where $P$ is load: (**a**) Mode I, (**b**) Mode II, and (**c**) Mode III.

shear loading in the crack plane (Mode II) and antiplane shear (Mode III), as defined in Figure 1. Only Mode I loading is considered herein.

### 2.1. Crack Tip Stresses

The simplest case for fracture mechanics analysis is a linear elastic material where stress, $\sigma$, is proportional to strain, $\epsilon$, giving

$$\sigma = E\epsilon \qquad (1)$$

where $E$ is the elastic modulus. In this case the stresses and strains around the tip of a sharp crack, for a given applied remote load, can be shown to vary inversely with the square root of the distance $r$ from the crack tip (16) and go to infinity precisely at the crack tip. This is most easily visualized by considering the distribution of stress around the end of the primary axis of an elliptical hole in an infinite plate, as shown in Figure 2. The $Y$ direction stress, $\sigma_Y$, along the $X$ axis can be written as (11):

$$\sigma_Y = \sigma[1 + a^{0.5}(2\rho + 2r)/(\rho + 2r)^{1.5}] \qquad (2)$$

for $\rho \ll a$, where $a$ is the primary axis length, $b$ is the minor axis, $\rho = b^2/a$, and $\sigma$ is the remotely applied stress on the system. As $b$ tends to zero, equivalent to the sharp crack case, $\sigma_Y$ goes to infinity exactly at the end of the crack and varies inversely with the square root of the distance $r$ from the end of the crack:

$$\sigma_Y = \sigma[1 + (a/2r)^{0.5}] \qquad (3)$$

Therefore, the magnitude of the stress at small distances from the crack tip is a function of the crack length, $a$, and the remotely applied stress, $\sigma$. Close to the crack tip ($r \ll a$) the stress can be scaled using a parameter

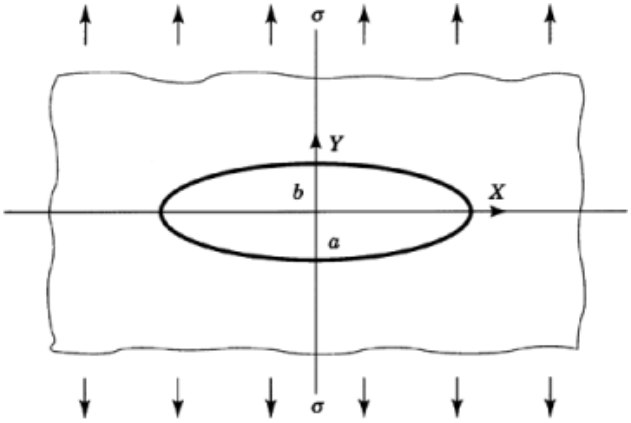


**Fig. 2.** An elliptical hole in a large plate where the arrows indicate the direction of stress. Terms are defined in text.

called the stress intensity factor, $K$ (9–11):

$$\sigma_Y = K/(2\pi r)^{0.5} \qquad (4)$$

where $K$ is a function of the nominal remotely applied stress in the uncracked body and the crack length:

$$K = \sigma Y a^{0.5} \qquad (5)$$

where $Y$ is a factor which corrects for different geometries and is a function of the size of the crack relative to the dimensions of the test specimen or cracked structure. For a crack in an infinite plate loaded in tension (the case considered here) $Y = \pi^{0.5}$. All of the stresses around the crack tip can be expressed in terms of $K$, and a more general form of equation 4 is

$$\sigma_\theta = (K/(2\pi r)^{0.5})\ [f\ (\theta)] \qquad (6)$$

Because the material is assumed to be linear elastic, the local displacements around the crack tip can also be expressed in terms of $K$.

Clearly the stresses and strains are not actually infinite in real materials, but it is found that in relatively brittle materials, where the amount of plastic yielding is small, failure is controlled by $K$ and fracture occurs when a critical value of $K$ is applied. This critical value is the fracture toughness of the material, denoted $K_{IC}$ where the subscript I indicates Mode I loading as shown in Figure 1. A zone of plastic yielding close to the crack tip prevents the stresses and strains from becoming infinite, but as long as this zone is small the overall toughness of the material can be characterized using $K_{IC}$.

### 2.2. Energy Release Rates

The analysis can equivalently be conducted in terms of the energy dissipated in growing the crack, rather than the stresses. The energy release rate, $G$, is the rate at which energy is released from the overall system as the crack grows. This is the energy released per unit area of crack surface formed, rather than a time-dependent rate, and so describes the energy available to drive the crack through the material. $G$ can be thought of as the energy which would be available to drive the crack if the crack were to grow at the current applied remote

stress level. In fact, the crack does not begin to grow until this available energy is sufficient to overcome the resistance of the material to crack growth. As for $K_{IC}$, there is a critical energy release rate, $G_{IC}$, at which the crack begins to grow. The two approaches are complementary and, by considering the rates of change of the stresses and displacements around the crack tip per unit of crack growth, it can be shown that for plane strain conditions (9–11):

$$K^2 = EG/\left(1-\nu^2\right) \qquad (7)$$

in general and

$$K_{IC}^2 = EG_{IC}/\left(1-\nu^2\right) \qquad (8)$$

in particular at fracture, where $\nu$ is Poisson's ratio. Therefore, $G$ can be expressed in terms of the applied remote stress and the crack length using equations 5 and 7 giving

$$G = \sigma^2 Y^2 a\left(1-\nu^2\right)/E \qquad (9)$$

$G$ can be calculated from the change in compliance, ie, the reciprocal of stiffness, of the structure or test specimen. For a cracked body of arbitrary shape loaded to a load $P$ and displacement $u$, as shown in Figure 3**a**, if some increment of crack growth, $\delta a$, occurs this leads to an increase in the compliance of the specimen, causing a reduction in the load, an increase in the displacement, or both. Referring to Figure 3**b,** the change in stored energy is the area $ABC$ and the work done by the applied load is $BCDE$. Hence, an expression for the change in total potential energy of the system, $U$, for an incremental change in load and displacement can be written (9–11):

$$\delta U = 0.5Pu - 0.5\left(P+\delta P\right)\left(u+\delta u\right) + \delta u\left(P+0.5\delta P\right) = 0.5\left(P\delta u - u\delta P\right) \qquad (10)$$

Because $G$ is defined as the energy released per unit area of crack surface formed, or more correctly the energy which would be released if the crack were to grow at the present applied load, then:

$$G = (1/B)\ (dU/da) = \left(P^2/2B\right)\ (dC/da) = 0.5B\left(u/C\right)^2 (dC/da) \qquad (11)$$

where $B$ is the thickness of the specimen, as shown in Figure 3, and $C$ is the compliance of the specimen. This relationship is useful for experimental determination of the energy release rate.

### 2.3. Crack Tip Yielding and Constraint

In any real material there is some plastic yielding at the crack tip, even though the overall fracture behavior of the material can be characterized using stress intensity concepts which consider the stresses in the elastic region. From the elastic solutions for the stresses close to the crack tip, for example equation 4 for the $Y$ direction stresses, and an appropriate yield criterion, such as that of von Mises (9–11), it is possible to calculate the size and shape of the plastically yielded zone at the crack tip. Figure 4**a** shows this zone schematically. The plastic zone is larger near the free surfaces of the specimen than at the center. This is because the high stresses and strains in the plane of the specimen (the $XY$ plane) lead to a tendency to contract laterally (in the $Z$ direction) at the crack tip. This can occur at the free surfaces, but near the center the unyielded material surrounding the crack tip tends to resist this contraction. A positive stress in the $Z$ direction is generated. Because yield criteria such as those of von Mises are based on the difference between the principal stresses in the three coordinate directions, this $Z$ direction stress acts to restrict the total amount of plastic yielding in

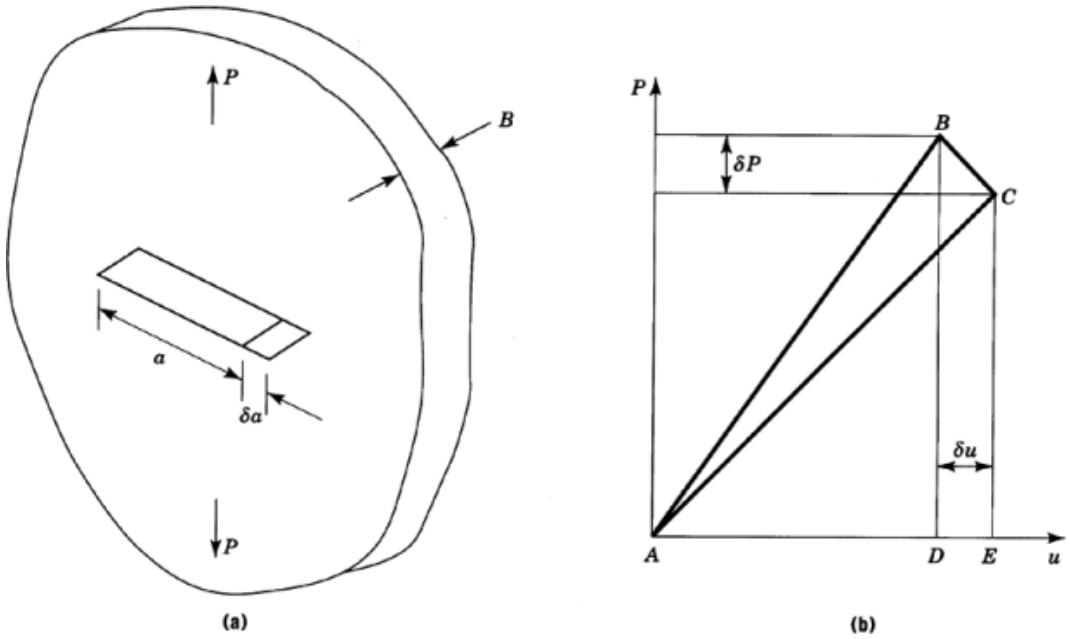


**Fig. 3.** The effect of crack growth on potential energy in a loaded body where (**a**) is a cracked body of arbitrary shape with a load $P$ applied, and (**b**) is the change in potential energy in the body owing to incremental crack growth, $\delta a$. Other terms are defined in text.

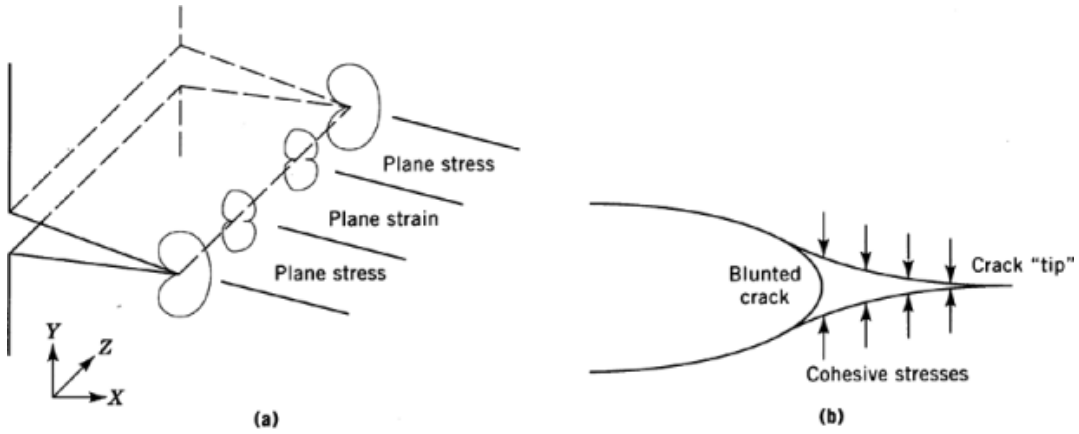


**Fig. 4.** (**a**) The crack tip plastic zone and (**b**) the Dugdale plastic zone model. Terms are defined in text.

the center of the specimen. The degree of constraint and the size of the plastic zone is approximately constant above some minimum distance into the specimen.

This constraint effect is the reason why there is a minimum specimen thickness requirement for valid fracture toughness testing. The plastic work done in the crack tip plastic zone as the crack grows is a significant part of the total work which must be done to grow the crack. For thin specimens, the size of this zone, and the total amount of work done, is a function of the thickness of the specimen. Therefore, the measured toughness is also a function of the thickness of the specimen. However, the true fracture toughness is a material property

independent of the test specimen geometry (including thickness) used to measure the value. This is only the case if a relatively thick test specimen is used. When the thickness is sufficient to generate $Z$ direction constraint, the toughness measured is referred to as the plane strain fracture toughness of the material, because deformation is largely confined to the $XY$ plane.

The distance from the crack tip, along the $X$-axis, at which the von Mises equivalent stress falls below the yield stress, defines the size of the plastic zone, $r_p$. For the plane stress case of unconstrained yielding, which corresponds to the free surface of the specimen in Figure 4, this gives

$$r_p = (1/2\pi)\ (K/\sigma_0)^2 \qquad (12)$$

where $\sigma_0$ is the yield stress of the material. This equation assumes a perfectly plastic material. In the center of the specimen the plastic zone is substantially smaller by an amount dependent on the Poisson's ratio of the material. An alternative estimate of the length of the plastic zone has been obtained (17) by treating the plastic zone as a cohesive zone, partially drawing the crack faces back together behind the effective crack front, as shown in Figure 4**b.** This leads to an expression of similar form to equation 12, although the constant is larger. This model is useful as it introduces the concept of crack tip blunting. Behind the cohesive zone the crack has opened out, and is no longer sharp, as a result of the plastic yielding that is occurring at the crack tip. The amount of blunting before crack growth occurs can be related to the energy needed to grow the crack, $G_{IC}$, and the yield stress of the material (9–11).

## 3. Elastic–Plastic Fracture Mechanics

In more ductile materials the assumptions of linear elastic fracture mechanics (LEFM) are not valid because the material yields more at the crack tip, so that the stresses and strains around the tip are no longer dominated by the linear elastic analysis. In order to characterize the fracture behavior of the material it is necessary to look inside the plastic zone at the distribution of stress and strain. If it is assumed that the material deforms in tension according to a power law hardening stress–strain curve,

$$\sigma = \sigma_0 \epsilon^n \qquad (13)$$

then it is possible to calculate the variation of stress and strain within the yielded crack tip zone. This stress and strain distribution is known as an HRR field (18–20). The magnitude of the product of stress and strain is characterized by a different parameter, the $J$-integral, and this product varies inversely with the distance from the crack tip, the same as in the linear elastic case. However, the individual variation of stress or strain alone is no longer the simple inverse square root form of the linear elastic case, but a more complex expression dependent on the shape of the stress–strain curve.

The $J$-integral derives its name from the fact that it is a contour integral which circles the crack tip. It describes the rate per unit area of crack surface at which energy would have to cross the integration path, or be released from strained material inside the integration path, in order to grow the crack. The value of $J$ obtained is independent of the path used to evaluate it in all regions that are characterized by the HRR stress field (18). The HRR field is only valid as long as the stresses and strains are proportional at the crack tip, ie, when strain increases stress also increases. Therefore, the $J$-integral only characterizes the crack tip stresses and strains in the region where this condition is met. The HRR analysis leads to a prediction of an infinite product of stress and strain precisely at the tip of a sharp crack, as with the elastic analysis. In practice, very close to the crack tip there is a region of reducing stress (unloading) owing to the blunting of the crack tip.

The parameters $K$, $G$, and $J$ are complementary and the relationship between them can be seen by considering the boundary between the beginning of the plastic zone and the surrounding elastic (unyielded)

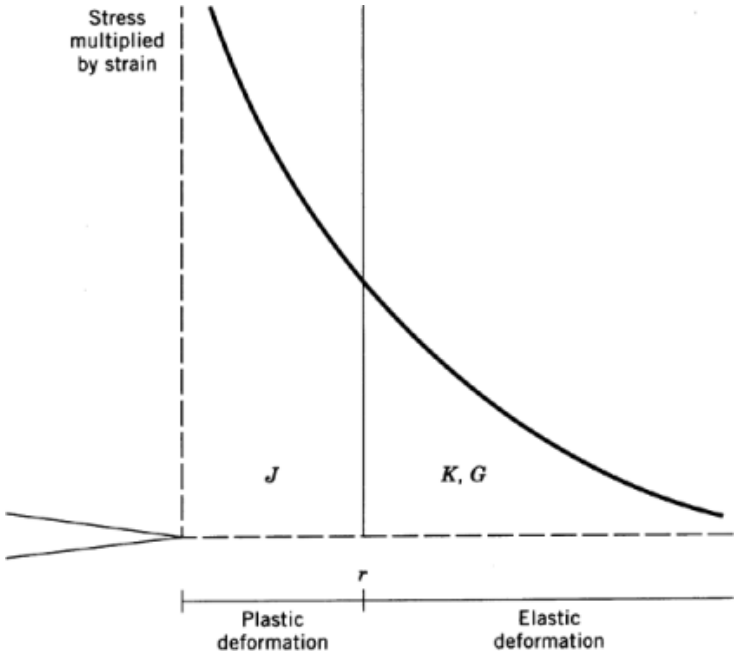


**Fig. 5.** The boundary between elastic and plastic zones at the crack tip. Terms are defined in text.

material, as shown in Figure 5. $J$ can also be used as a measure of the toughness of a material, like $K_{IC}$, by defining a critical value $J_{IC}$ (5), or by plotting the applied $J$ to produce various amounts of crack growth (6). The magnitude of the blunting at the crack tip resulting from local yielding can be quantified using the crack-opening displacement (COD), which is defined as the separation of the crack faces at the points where two lines drawn back from the crack tip at 45° to the crack path intersect the crack faces. The COD is proportional to the applied $J$-integral and inversely proportional to the yield stress of the material. The proportionality constant is dependent on the shape of the stress–strain curve of the material (18). The COD has been proposed as a fracture criterion on the basis that crack growth begins when a critical COD value is reached (9).

## 4. Micromechanisms

For a perfectly brittle material the fracture process involves the breaking of bonds at an atomic level to form new surfaces. This was the original concept (1) and was based on studies of the fracture of glass (qv). The energy needed per unit area of new surface formed, $\gamma$, was considered. Because the growth of a crack forms two new surfaces, the energy release rate needed to drive the crack in a brittle material is $2\gamma$. However, in most engineering materials there is also a significant amount of plastic energy which must be dissipated in order to grow the crack, which gives a condition for crack growth of the form:

$$G \text{or} J = \left(2\gamma + W_p\right) \qquad (14)$$

where $W_p$ is the plastic work that must be done to grow the crack. Fracture mechanics attempts to quantify the amount of energy needed to grow the crack, by treating the behavior on a macroscale continuum basis. The objective is to subtract all nonessential work done in deforming the test specimen to determine the energy

specific to the crack growth process alone. Locally at the crack tip various microscale processes are occurring to actually fail the material (21). There is some process zone, inside the plastic zone adjacent to the blunted crack tip, where material has been deformed so much that it begins to rupture. Examples of the mechanisms occurring in the process zone are cleavage along grain boundaries or void growth and coalescence in metals (9, 10). In some polymers crazing may occur owing to the triaxial stresses at the crack tip (11, 22). It is often possible to get some information about the fracture behavior from the appearance of the fracture surface after the crack has grown.

## 5. Practical Testing Procedures

### 5.1. Specimen Requirements

Fracture toughness tests divide into two distinct groups, $K_{IC}$ (or $G_{IC}$) measurements for relatively brittle materials and $J$-integral tests for more ductile materials. The reason for this becomes apparent when the $K_{IC}$ test is considered. Fracture mechanics testing is required to follow certain procedures so that a valid measurement is obtained. Specifically, the initial crack in the test specimen must be sharp and the thickness and depth of the specimen must be sufficient to generate the plane strain constraint discussed earlier. A poorly conducted fracture mechanics test leads to an overestimate, rather than an underestimate, of the true toughness of the material. Hence, care is needed to ensure a valid measurement. Basically a thick specimen is always preferable to a thin specimen, but if the available material thickness is limited, then a test can be conducted to determine a provisional toughness $K_Q$. Using the yield stress of the material, $\sigma_0$, an assessment can then be made of the validity of $K_Q$ using the expression

$$B_{\min}, (D-a)_{\min}, a_{\min} = 2.5\left(K_Q/\sigma_0\right)^2 \qquad (15)$$

where $B_{\min}$ is the minimum specimen thickness to obtain a valid measurement for a material with that toughness and yield stress, $(D-a)_{\min}$ is the minimum uncracked ligament in the direction of crack growth, and $a_{\min}$ is the minimum initial crack length. For example, if $B_{\min}$ is greater than the specimen thickness that was actually used to measure $K_Q$, then $K_Q$ is, unfortunately, not a valid measurement and a thicker specimen is needed to generate the plane strain constraint. Sidegrooves can sometimes be used to generate additional constraint so that a valid measurement can be obtained with a restricted thickness. However, this complicates the calculation of the toughness (23).

In tougher materials the minimum thickness required by equation 15 can become excessive. In such cases the $J$-integral test is an attractive alternative. Because this test considers the stress distribution around the crack inside the plastic zone, it can be used to obtain a valid toughness measurement in a thinner specimen, because more extensive plastic yielding does not invalidate the analysis. The equivalent of equation 15 for the $J$-integral test is

$$B_{\min}, (D-a)_{\min}, a_{\min} = 25\left(J_Q/\sigma_0\right) \qquad (16)$$

where $J_Q$ is a provisional value of $J_{IC}$.

The other important point is to achieve a sharp initial crack or notch. The initial notch is typically about half the depth of the specimen and a pre-notch is usually sawn or machined into the specimen. This notch must be sharpened. In metals this is often done by cycling the specimen in fatigue loading at a low load to grow a natural crack some distance beyond the machined notch (9). In other materials, such as polymers, a sharp crack can be achieved by skillfully sharpening the crack tip using a new razor blade (11). Although fracture

toughness tests can be conducted at any loading rate, most are done at low rates such as a cross-head rate of 10 mm/min, using a suitable screw driven or servohydraulic load frame.

### 5.2. Fracture Toughness Testing

Some typical fracture toughness test geometries are shown in Figure 6. The single-edge notch (SEN) or center notch (CN) specimens are loaded in tension. The compact tension (CT) specimen applies an opening load to the crack, using pins loading through holes in the specimen. The three-point bend (TPB) specimen is supported at each end and loaded downward at the center opposite the notch. Different calibration factors ($Y$ in eq. 5) are tabulated for the different geometries so that the applied stress intensity can be calculated from the load at fracture and the crack length. To obtain valid plane strain fracture toughness values the ASTM standards (4, 7) set certain requirements for the dimensions of the specimen.

A fracture toughness test, where unstable brittle fracture occurs at a critical applied load, leads to a load–displacement curve like that shown schematically in Figure 7**a,** having an essentially linear loading curve and a catastrophic drop in load at fracture. Gross nonlinearity in the loading curve generally indicates that excessive yielding is occurring, although it may also indicate slow stable crack growth prior to unstable fracture. Because it is the fracture toughness at the initiation of crack growth that is desired, the load at this point must be determined. The ASTM standards suggest drawing a line through the straight part of the loading curve and then drawing a second line $AB$ with a 5% lower slope, as shown in Figure 7**b.** If the maximum load falls between these lines, then this load is used to calculate the toughness of the material. If the maximum load is outside these lines, then a reduced load at the point where the 95% slope line crosses the loading curve should be used. Other conditions must also be met, as described in the standards. If the reduced load is less than 90% of the maximum load, or if brittle fracture does not occur, then the test is invalid and a $J$-integral test must be considered. Some typical $K_{IC}$ values in units of $\mathrm{MPa\sqrt{m}}$ are steel, 40–90; titanium, 38; aluminum, 30; 30% glass-reinforced nylon-6,6, 6.0; nylon-6,6, 3.5; ABS resins, 2.0; poly(methyl methacrylate) (PMMA), 1.2; and epoxies, 0.6.

### 5.3. *J*-Integral Testing

The $J$-integral test is rather different from the $K_{IC}$ test because a curve of crack growth resistance against crack growth is generated (24). An example of such a curve is shown schematically in Figure 8. This requires more than one specimen, with each specimen loaded to different levels to generate different amounts of crack growth (5). After the test each specimen is broken open, for example by cooling in liquid nitrogen and impacting at a high rate to generate brittle failure, and the amount of crack growth is measured from the appearance of the fracture surface. The crack front typically has some curvature. More crack growth occurs in the center of the specimen, so that either an average crack growth can be obtained by taking a number of measurements across the thickness (5), or the maximum crack growth can be used, which leads to a conservative estimate of toughness. This curvature arises from the plane strain conditions at the center of the specimen and the higher apparent toughness plane stress state at the surface. The corresponding applied $J$ is calculated from the input energy, the area under the load–deflection curve, using an equation of the form

$$J = 2U/\,[B\,(D - a)] \qquad (17)$$

where $B$, $D$, and $a$ are the specimen thickness, depth, and crack length, respectively. This equation is only valid when certain constraints on specimen dimensions are met (6, 10). The resistance curve can be then be constructed by plotting the applied $J$ values against the resulting crack growth. The standards (5, 6) set requirements for the number and spacing of the data points used to construct the curve. An alternative single-specimen method uses just one specimen, which is progressively loaded to higher and higher loads (higher

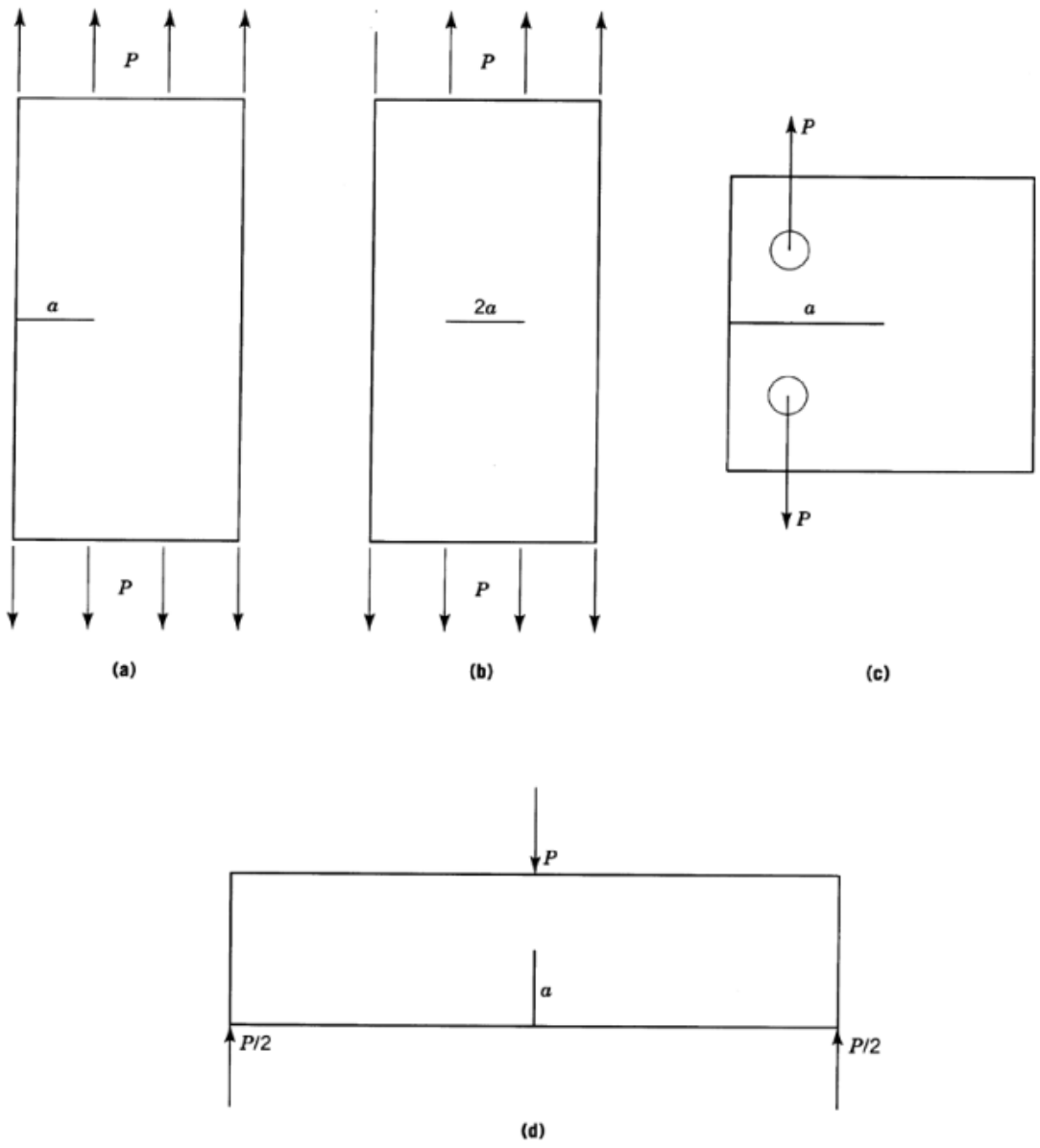


**Fig. 6.** Fracture toughness test specimens: (**a**) single-edge notch; (**b**) center notch; (**c**) compact tension; and (**d**) three-point bend. Terms are defined in text.

applied $J$ values), partially unloading the specimen between each increment of load increase. From the slope of the partial unloading curves the compliance of the specimen is obtained and the crack length is calculated from this compliance (6). The resistance curve can then be constructed from the area under the curve up to each partial unloading point and the corresponding crack growth.

An attempt has been made to define a single critical $J_{IC}$ value, like $K_{IC}$ for brittle fracture, from these curves (5). However, the amount of crack growth which is used to define this critical value is inevitably rather

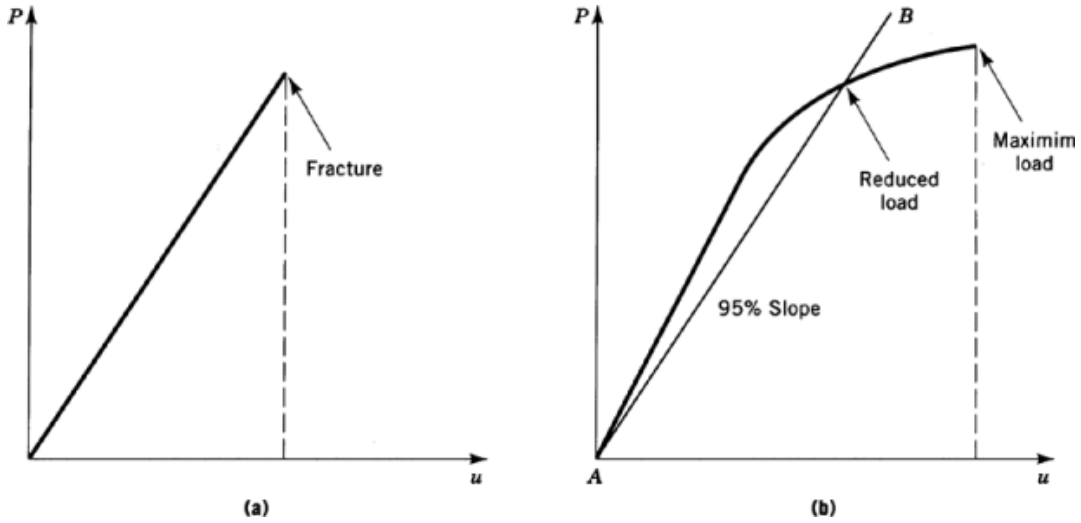


**Fig. 7.** Load versus deflection for (**a**) perfectly brittle fracture and (**b**) slight nonlinearity. Terms are defined in text.

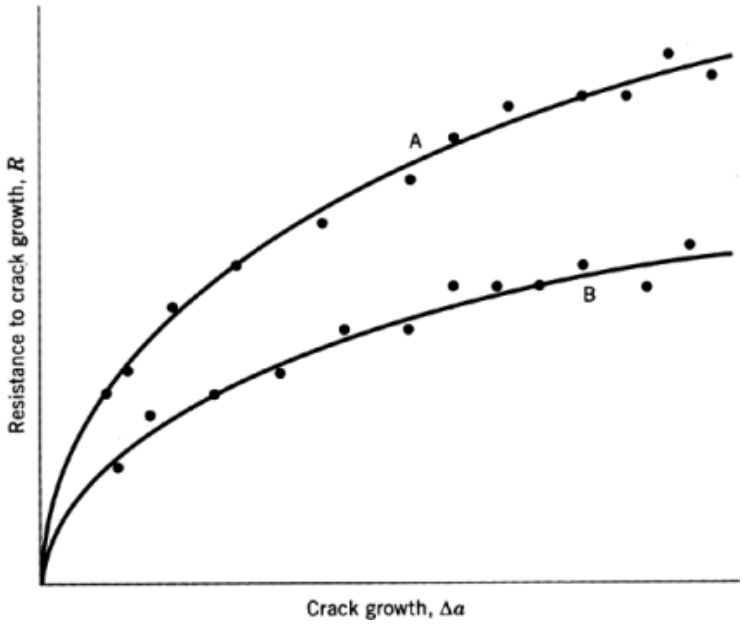


**Fig. 8.** *J*-integral test resistance curves for materials A and B.

arbitrary. A more recent approach (6) is to fit a power law curve of the form

$$J = A\,(\Delta a)^n \qquad (18)$$

to the data, where $\Delta a$ is the measured crack growth and the coefficients $A$ and $n$ can be used for relative comparison of materials. A material having a higher resistance curve, ie, more energy per unit of crack growth,

is nominally tougher, but full interpretation of these curves is rather complex because the slope of the curve must also be considered, relative to the system applying the load, to assess the stability of the crack. Because the resistance curve of material A in Figure 8 is always above that of material B, then material A is the tougher of the two.

## 6. Fatigue

Fatigue cracking is slow crack growth under repeated cyclic loading or constant static load. For cyclic loading unnotched fatigue data are often presented in the form of *S–N* curves, where applied stress, *S,* is plotted against cycles to failure, *N.* This method leads to widely scattered data because the total lifetime is the sum of the time to initiate a crack from an existing inherent flaw, the size of which is variable between specimens, and the time to grow the crack to final failure of the specimen. This variability is overcome by using fracture mechanics because a deliberate initial crack is introduced into the specimen, which is then cyclically loaded. Because the load applied to each cycle is generally quite low, relative to the single-cycle failure load, the amount of plastic yielding at the crack tip should not be excessive and the problem is well suited to characterization using linear elastic fracture mechanics (LEFM) (25). For cyclic loading between some maximum and minimum load, the corresponding maximum and minimum applied $K$ can be calculated, provided the length of the crack is continually monitored during the test. Data can then be plotted in the form of the rate of change of crack length per cycle, *da/dN,* against the range of applied $K$ per cycle, $\Delta K = (K_{\max} - K_{\min})$. A $da/dN$ curve such as that shown schematically in Figure 9 is generally obtained, consisting of three regions. The first region is a slower growth rate at small applied $\Delta K$ levels, with the possibility of a threshold $\Delta K$ below which no crack growth at all occurs. The main crack growth is described by the Paris law (26):

$$da/dN = D\,(\Delta K)^m \qquad (19)$$

and the final region is more rapid crack growth at higher applied $\Delta K$ levels. A log–log plot of the main crack growth data allows the constants $D$ and $m$ in equation 19 to be estimated. It is then possible to integrate equation 19 to predict the number of cycles for a crack to grow from some initial length to a final length. However, some caution is needed in making such a calculation because there are many variables in fatigue behavior that must be considered. In particular, the ratio of the maximum applied stress to the minimum stress during each cycle is an important parameter. This ratio is called the cycle or $R$ ratio. A unique curve of the form described by equation 19 is only obtained for a constant $R$ ratio, because the same $\Delta K$ can be applied for any $R$ value. Therefore, it is more complete to write

$$da/dN = f\,(\Delta K, R) \qquad (20)$$

The conditions at the crack tip during fatigue loading can be quite different, depending on the $R$ ratio. For example, if the $R$ ratio is negative then the crack is forced closed during part of the cycle. The stress intensity calculation has no meaning when the applied loading is compressive, and it could be argued that the crack growth rate is then controlled by the tensile loading part of the cycle alone. However, there is a plastic zone at the crack tip, so that the crack does not close perfectly as soon as the applied loading becomes negative, which means that the compressive part of the loading also makes some contribution to the generation of damage at the crack tip. Provided the experimental data have been obtained at the appropriate $\Delta K$ and $R$ for the application where fatigue life is to be predicted, then an allowance for these factors can be incorporated in the data. Further complications can arise if the component or structure being analyzed experiences random loadings of different severity during its service life. The prediction of total fatigue life is then dependent to some extent on the sequence in which these different amplitude loadings occur. An overload cycle, above previous

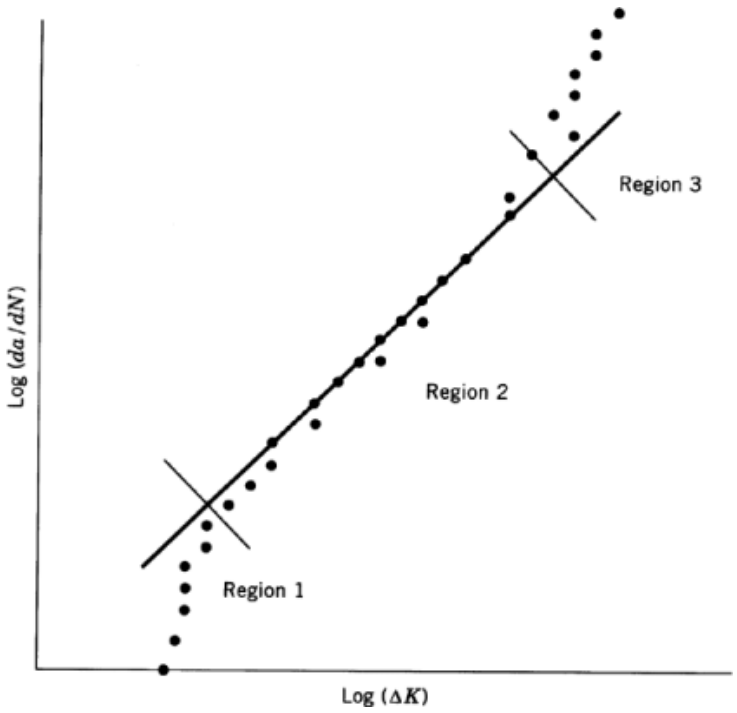


**Fig. 9.** Schematic fatigue crack growth data showing the regions of growth rate.

applied stress intensity levels, generates compressive residual stresses at the crack tip which inhibit crack growth when the applied stress intensity reduces to its original range in subsequent cycles (27). Therefore, a simple analysis based on integrating equation 19 to determine the lifetime gives a conservative prediction (an overestimate of the growth rate) by ignoring the interaction between cycles of different amplitude. This is a topic for more specialized texts (10, 28). Equation 19 provides the powerful capability to estimate the number of cycles needed for a crack to grow some amount. By periodically monitoring the length of fatigue cracks in structures such as pressure vessels and aircraft, and considering $da/dN$ data, a decision can be made about whether it is safe for the structure to remain in service until the next inspection.

Fracture mechanics concepts can also be applied to fatigue crack growth under a constant static load, but in this case the material behavior is nonlinear and time-dependent (29, 30). Slow, stable crack growth data can be presented in terms of the crack growth rate per unit of time against the applied $K$ or $J$, if the nonlinearity is not too great. For extensive nonlinearity a viscoelastic analysis can become very complex (11) and a number of schemes based on the time rate of change of $J$ have been proposed (31, 32).

The measurement of crack length in a laboratory specimen can be achieved using various methods. The surface of the specimen can be observed with a traveling microscope to measure the apparent growth. In metals a method based on the changing electrical resistance of the specimen, resulting from the growth of the crack, can be used (9, 33). Ultrasonic techniques (9) can also be used , or the crack length can be deduced by calculation from measurements of the compliance of the specimen and the applied load (34). An ASTM standard for fracture mechanics fatigue testing has been prepared (35). Restrictions on the specimen dimensions for a valid test apply, of similar form to equation 15. However, for fatigue testing there is a maximum specimen thickness, rather than a minimum thickness, because of concerns about the curvature of the crack front and also the possibility of heat generation inside the specimen during cycling. Heat generation is of particular

concern in testing polymers where the thermal conductivity is low and where viscoelastic effects may cause significant heat generation (11, 36, 37). Heating can be reduced by lowering the frequency of the cyclic loading, which is typically in the range of 1–5 Hz.

## 7. Impact Loading

The fracture toughness of a material can vary with the strain rate at which the test is conducted. This is why materials such as polymers tend to be more brittle when loaded rapidly. For this reason, fracture mechanics tests are also conducted under impact loading conditions. The three-point bend specimen is probably the most commonly used geometry for impact tests. A falling weight with a suitable loading head is released from a measured height so that it impacts the back of the specimen at a known speed. In principle the fracture toughness can be calculated as before, using an equation of the form of equation 5 and the load at fracture. In practice, as the loading rate increases, dynamic vibration of the specimen occurs during loading, after the initial impact, and the load–displacement signal recorded by a transducer attached to the impacting head tends to show substantial oscillations. This makes it difficult, if not impossible, to determine the load at fracture accurately (38). Alternative approaches, such as measuring the displacement to failure rather than the load, may be necessary (39).

The commonly used Izod test and Charpy test, for example, as described in the ASTM standards for metals and polymers (40, 41) (see also Plastics testing), are not fracture mechanics tests for a number of reasons. First, a blunt notch is used, whereas in a fracture mechanics test a sharp notch is of vital importance. Second, the total energy to fail the specimen, rather than the energy specific to the crack growth process, is recorded. Third, no account is taken of the plane stress–plane strain effects discussed earlier. Therefore, for a constant specimen thickness, two different materials having similar fracture toughnesses but different yield stresses may record different performances in an Izod or Charpy test, simply because one material happens to be in plane stress and the other in plane strain at that specimen thickness. However, a fracture mechanics variation on the basic Charpy test is possible for materials where LEFM is valid. If a series of impact tests are performed on Charpy-type three-point bend specimens with sharp notches and a range of initial crack lengths, then the energy to break can be plotted against a function of the compliance of the specimen. It can be shown (11) that:

$$G_{IC} = U/BD\phi \qquad (21)$$

where $G_{IC}$ is the critical plane strain energy release rate, $U$ is the energy to break the specimen, $B$ and $D$ are the thickness and depth of the specimen, respectively, and $\varphi$ is a rather complex function of the compliance of the specimen, which depends on its dimensions, including the crack length. Therefore, by plotting $U$ against $BD\varphi$ for a range of initial notch lengths, a straight line should be obtained having a slope equal to the critical energy release rate of the material. As for other fracture toughness tests, care must be taken to check that the thickness of the specimen is sufficient for a valid measurement.

## 8. Dynamic Crack Propagation

In the preceding sections the measurement of fracture toughness for a stationary crack was considered. The load up to fracture may be applied slowly or rapidly, as in an impact test, but the crack itself is not moving until fracture occurs. The more rapidly the load is applied, the higher the strain rate around the crack tip. Hence, some dependence of fracture toughness on loading rate is generally observed. Therefore, it is to be expected that the fracture toughness of a material where the crack is propagating at some speed also varies with the

speed at which the crack is growing. Because the toughness of a material tends to fall with increasing rate, up to some limit, once a crack begins to propagate in an unstable manner it accelerates to a high (over 100 m/s) speed. Therefore, the calculation of the fracture toughness becomes an extremely complex problem, as the available energy to drive the crack is controlled by dynamic effects. Specialized techniques are needed to calculate the energy release rate during rapid crack propagation (42, 43) and to measure the fracture toughness experimentally (44, 45). It may appear that such calculations are of rather academic interest, because the structure has apparently failed if the crack is running at such speeds. However, there is considerable interest in understanding dynamic fracture problems to determine the conditions for a rapidly propagating crack to arrest before total failure occurs (46). For example, in continuous steel or polyethylene pipelines (qv) there is the worrisome possibility that a crack which started to propagate could run along the axis of the pipe for a large distance, perhaps driven by gas pressure inside the pipe. Dynamic fracture has, therefore, received considerable attention in terms of both theoretical and experimental investigations.

## 9. Environment and Temperature

All of the tests discussed herein could be conducted at different temperatures and in different environments. The effect of a particular environment or temperature can be significant and the experimenter should take care to ensure that the data is collected under the appropriate conditions for the problem being considered. When testing at elevated temperatures it is important to check the validity of the measurement using equation 15, based on a yield stress measured at the temperature of the fracture toughness test. Stress corrosion cracking is the term used for the combined effect of an aggressive environment and an applied stress on the propagation of a crack (47). In the case of metals the effect may be either erosion of material at the crack tip in an anodic process, or the evolution of hydrogen in a cathodic process which then diffuses into the metal and causes hydrogen embrittlement (9, 48). For polymers, solvents that diffuse very slowly into the polymer when it is not loaded may enter the crack tip region quite rapidly when a stress is applied, probably because of the formation of voids or crazes under load. The solvent then plasticizes the crack tip, leading to a deterioration of properties and more rapid crack growth (11). The variety of combinations of materials, environments, and potential interactions is so great that any fracture toughness measurement must be performed in the environment in which the component being designed is to be used.

## 10. Applications and Design Issues

Fracture toughness is often used purely as a relative comparison of the cracking resistance of different materials. However, it has the potential to also be used for quantitative prediction of actual component or structure performance. If the size of the crack or inherent flaw present in a component can be determined, then by performing a stress analysis of the structure, probably by finite element analysis (49), or referring to tabulated stress intensity factor solutions for different geometries (50, 51), it is possible to calculate the applied stress intensity loading on the crack for a particular load on the structure. In a complex three-dimensional structure, substantial computational effort may be needed to accurately determine the applied stress intensity. A crack growing from a defect generally has a curved crack front profile, eg, a penny-shaped crack, unlike the straight crack, two-dimensional laboratory specimens considered herein. This complicates the calculation of applied stress intensity. However, once the applied stress intensity at the design load has been determined, an assessment of whether fracture will occur can be made. A number of rather elaborate design procedures have been developed, one of which is the R6 design code (52, 53). This design procedure essentially considers the two competing failure processes of gross plastic yielding across the uncracked cross section, leading to failure

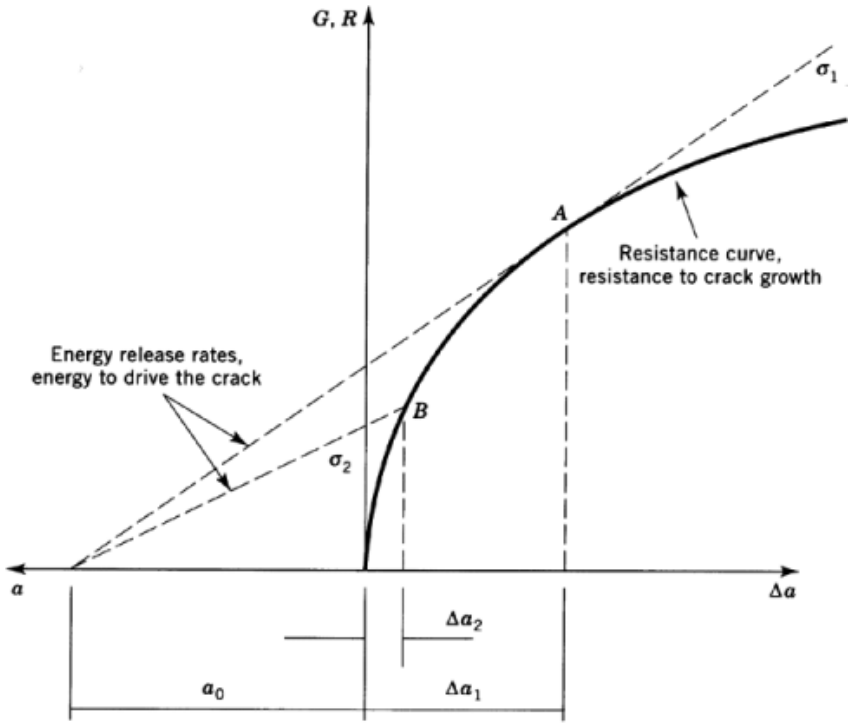


**Fig. 10.** Stability of a crack in a structure. See text.

by plastic collapse of the structure, and failure by crack growth. It attempts to define combinations of these two modes which would lead to failure when neither alone would be sufficient.

For a crack growing under $J$-integral controlled conditions in a structure, the crack may grow some distance and then stop, or it may propagate unstably. To determine the stability of a crack in a structure it is necessary to know the form of the resistance curve of the material and also the energy which could be released from the structure to drive the crack. A construction of the form shown schematically in Figure 10 can be used to assess stability. The energy release rate of the structure is proportional to the crack length, for a given applied stress (from eq. 9), whereas the energy needed for an amount of crack growth $\Delta a$ follows the resistance curve. The tangent point *A,* for a particular initial crack length $a_0$ and applied stress $\sigma_1$, defines the transition from stable crack growth to unstable fracture. For a lower applied stress $\sigma_2$ the crack grows some amount, up to point *B,* and then stops without instability occurring. Note that $a_0$ is much greater than $\Delta a$ and Figure 10 is not drawn to scale. For a brittle material characterized with $G_{IC}$, the resistance curve would be a horizontal line at $G_{IC}$ on the $Y$ axis. As soon as the applied energy release rate was equal to $G_{IC}$, unstable fracture would occur. Brittle materials have a flat resistance curve.

The use of fatigue data and crack length measurements to predict the remaining service life of a structure under cyclic loading is possibly the most common application of fracture mechanics for performance prediction. In complex structures the growth of cracks is routinely monitored at intervals, and from data about crack growth rates and the applied loadings at that point in the structure, a decision is made about whether the structure can continue to operate safely until the next scheduled inspection.

### 10.1. Nomenclature

| | |
|---|---|
| $a$ | length |
| $B$ | specimen thickness |
| $C$ | specimen compliance |
| COD | crack opening displacement |
| $D$ | specimen depth in the direction of crack growth |
| $E$ | elastic modulus |
| $G$ | energy release rate |
| $G_{IC}$ | plane strain critical value of $G$ |
| HRR | Hutchinson, Rice, and Rosengren |
| $J$ | $J$-integral value |
| $J_{IC}$ | plane strain critical value of $J$ |
| $K$ | stress intensity factor |
| $K_{IC}$ | plane strain fracture toughness |
| LEFM | linear elastic fracture mechanics |
| $N$ | number of cycles |
| $P$ | load |
| $r$ | distance from the crack tip |
| $r_p$ | plastic zone radius |
| $R$ | ratio of maximum to minimum stress in fatigue, or resistance to crack growth in $J$-integral testing |
| $u$ | displacement |
| $U$ | energy |
| $W_p$ | plastic work |
| $Y$ | geometric correction factor in the $K$ equation |
| $\gamma$ | surface energy |
| $\delta$ | crack opening displacement |
| $\Delta a$ | crack growth |
| $\epsilon$ | strain |
| $\nu$ | Poisson's ratio |
| $\sigma$ | stress |
| $\sigma_Y$ | stress in $Y$ direction |
| $\sigma_0$ | yield stress |
| $\varphi$ | energy calibration factor |

## BIBLIOGRAPHY

### Cited Publications


1. A. A. Griffith, *Phil. Trans. Roy. Soc.* **A221**, 163 (1920).
2. K. B. Broberg, *Eng. Fract. Mechanics* **16**, 497 (1982).
3. J. M. Barsom, *Fracture Mechanics Retrospective—Early Classic Papers (1913–1965)*, ASTM Publications, Philadelphia, 1987.
4. ASTM E399-90, "Plane Strain Fracture Toughness of Metallic Materials," *Annual Book of ASTM Standards*, ASTM Publications, Philadelphia, 1993.
5. ASTM E813-89, $J_{IC}$, "A Measure of Fracture Toughness," *Annual Book of ASTM Standards*, ASTM Publications, Philadelphia, 1993.

6. ASTM E1152-87, "Determining J–R Curves," *Annual Book of ASTM Standards*, ASTM Publications, Philadelphia, 1993.
7. ASTM D5045-91, "Plane Strain Fracture Toughness and Strain Energy Release Rate of Plastic Materials," *Annual Book of ASTM Standards*, ASTM Publications, Philadelphia, 1993.
8. J. G. Williams and M. J. Cawood, *Polym. Testing* **9**, 15 (1990).
9. J. F. Knott, *Fundamentals of Fracture Mechanics*, Butterworths, London, 1979.
10. D. Broek, *Elementary Engineering Fracture Mechanics*, Martinus Nijhoff, Dordrecht, the Netherlands, 1987.
11. J. G. Williams, *Fracture Mechanics of Polymers*, Ellis Horwood, Chichester, UK, 1984.
12. D. Broek, *The Practical Use of Fracture Mechanics*, Kluwer Academic Publishers, Dordrecht, the Netherlands, 1989.
13. K. Friedrich, *Application of Fracture Mechanics to Composite Materials*, Elsevier Science Publishers, Amsterdam, the Netherlands, 1989.
14. M. F. Kanninen and C. H. Popelar, *Advanced Fracture Mechanics*, Oxford University Press, New York, 1985.
15. R. W. Hertzberg, *Deformation and Fracture Mechanics of Engineering Materials*, John Wiley & Sons, Inc., New York, 1983.
16. M. L. Williams, *J. Appl. Mechanics* **28**, 109 (1957).
17. D. S. Dugdale, *J. Mechanics Phys. Solids* **8**, 100 (1960).
18. J. R. Rice and G. F. Rosengren, *J. Mechanics Phys. Solids* **16**, 1 (1968).
19. J. W. Hutchinson, *J. Mechanics Phys. Solids* **16**, 13 (1968).
20. *Ibid.*, p. 337.
21. S. Murakami, *JSME Int. J.* **30**, 701 (1987).
22. E. Passaglia, *J. Phys. Chem. Solids* **48**, 1075 (1987).
23. C. N. Freed and J. M. Krafft, *J. Mater.* **1**, 770 (1966).
24. W. Schmitt and R. Kienzler, *Eng. Fract. Mechanics* **32**, 409 (1989).
25. R. J. Allen, G. S. Booth, and T. Jutla, *Fatigue Fract. Eng. Mater. Struct.* **11**, 45 (1988).
26. P. C. Paris, M. P. Gomez, and W. E. Anderson, *Trend Eng.* **13**, 9 (1961).
27. D. J. Smith and S. J. Garwood, *Int. J. Pressure Vessels Piping* **41**, 255 (1990).
28. ASTM STP 462, *Effects of Environment and Complex Load History on Fatigue Life*, ASTM Publications, Philadelphia, 1968.
29. H. P. Van Leeuwen, *Eng. Fract. Mechanics* **9**, 951 (1977).
30. D. W. Rees, *Progr. Nucl. Energy* **19**, 211 (1987).
31. *Fracture Mechanics*, ASTM STP514, ASTM STP514, ASTM Publications, Philadelphia, 1972.
32. A. G. Atkins and Y-W. Mai, *Elastic and Plastic Fracture*, Ellis Horwood, Chichester, U.K., 1985.
33. K. J. Miller, *Proc. Inst. Mech. Eng., Part C: Mech. Eng. Sci.* **205**, 291 (1991).
34. A. Saxena and E. J. Hudak, *Int. J. Fract.* **14**, 453 (1978).
35. ASTM E647-93, "Measurement of Fatigue Crack Growth Rates," *Annual Book of ASTM Standards*, ASTM Publications, Philadelphia, 1993.
36. R. W. Hertzberg and J. A. Manson, *Fatigue of Engineering Plastics*, Academic Press, New York, 1980.
37. J. A. Sauer and G. C. Richardson, *Int. J. Fract.* **16**, 499 (1980).
38. R. A. Mines, *Int. J. Impact Eng.* **9**, 441 (1990).
39. J. G. Williams and G. C. Adams, *Int. J. Fract.* **33**, 209 (1987).
40. ASTM E23-93, "Notched Bar Impact Testing of Metallic Materials," *Annual Book of ASTM Standards*, ASTM Publications, Philadelphia, 1993.
41. ASTM D256-92, "Impact Resistance of Plastics and Electrical Materials," *Annual Book of ASTM Standards*, ASTM Publications, Philadelphia, 1993.
42. A. N. Atluri and T. Nishioka, *Int. J. Fract.* **27**, 245 (1985).
43. T. Nakamura, C. F. Shih, and L. B. Freund, *Int. J. Fract.* **27**, 229 (1985).
44. J. F. Kalthoff, *Int. J. Fract.* **27**, 277 (1985).
45. J. Duffy and C. F. Shih in K. Salama and co-workers, eds., *Proceedings of the Seventh International Conference on Fracture (ICF7)*, Pergamon Press, Oxford, U.K., Vol. **5**, (1989), p. 633.
46. E. J. Ripling and P. B. Crosley, *Eng. Fract. Mechanics* **23**, 21 (1986).
47. K. Sieradzki and R. C. Newman, *J. Phys. Chem. Solids* **48**, 1101 (1987).
48. R. P. Gangloff, *Mater. Sci. Eng.* **A103**, 157 (1988).

49. S. N. Atluri, *Computational Methods in the Mechanics of Fracture*, Elsevier Science Publishers, Amsterdam, the Netherlands, 1986.
50. D. P. Rooke and D. J. Cartwright, *Compendium of Stress Intensity Factors*, Her Majesty's Stationery Office, London, 1974.
51. Y. Murakami, ed., *Stress Intensity Factors Handbook*, Pergamon Press, Oxford, U.K., 1987.
52. I. Milne, R. A. Ainsworth, A. R. Dowling, and A. T. Stewart, *Int. J. Pressure Vessels Piping* **32**, 3 (1988).
53. S. T. Rolfe and J. M. Barsom, *Fracture and Fatigue Control in Structures*, Prentice-Hall, Inc., Englewood Cliffs, N.J., 1977.

BARRY A. CROUCH
E. I. du Pont de Nemours & Co., Inc.

## Related Articles

Composite materials